ELSEVIER

Sensors and Actuators A 101 (2002) 62–68

SENSORS AND ACTUATORS A PHYSICAL

www.elsevier.com/locate/sna

High electric field performance of $Al_{0.3}Ga_{0.7}As/GaAs$ and $Al_{0.3}Ga_{0.7}As/GaAs/In_{0.3}Ga_{0.7}As$ quantum well micro-Hall devices

Vasyl P. Kunets[a,*], Wolfgang Hoerstel[a], Helmar Kostial[b], Heiko Kissel[c], Uwe Müller[a], Georgiy G. Tarasov[d], Yuriy I. Mazur[e], Zoryana Ya. Zhuchenko[d], William Ted Masselink[a]

[a]*Department of Physics, Humboldt-Universität zu Berlin, Invalidenstrasse 110, 10115 Berlin, Germany*
[b]*Paul-Drude-Institut für Festkörperelektronik, Hausvogteiplatz 5-7, 10117 Berlin, Germany*
[c]*Ferdinand-Braun-Institut für Höchstfrequenztechnik, Albert-Einstein-Strasse 11, 12489 Berlin, Germany*
[d]*Institute of Semiconductor Physics, National Academy of Sciences, Prospect Nauki 41, 03028 Kiev, Ukraine*
[e]*Department of Physics, University of Arkansas, Fayetteville, AR 72701, USA*

Received 11 April 2002; accepted 13 May 2002

Abstract

Quantum well micro-Hall devices based on uniformly Si-doped $Al_{0.3}Ga_{0.7}As/GaAs$ and Si-δ-doped $Al_{0.3}Ga_{0.7}As/GaAs/In_{0.3}Ga_{0.7}As$ heterostructures are investigated as function of electric field and compared in terms of sensitivity and noise properties. The data show that at high electric fields, doped-channel quantum well devices are advantageous over high-mobility structures and that the use of pseudomorphic InGaAs results in better performance than does GaAs. A maximal signal-to-noise sensitivity (SNS) of 138 dB T^{-1} is achieved in a 10 μm × 10 μm device at 300 K, at frequency of 100 kHz and bandwidth of 1 Hz. This performance corresponds to a lowest detection limit of 127 nT $Hz^{-1/2}$, with no degradation for electric fields up to 2.4 kV cm^{-1}; these values represent the best reported at such high electric fields. Furthermore, our results suggest that a signal-to-noise sensitivity of 160 dB T^{-1} and a lowest detection limit of 10 nT is achievable in doped-channel structures.
© 2002 Elsevier Science B.V. All rights reserved.

PACS: 85.30.Fg; 73.50.Td; 72.80.Ey

Keywords: Hall device; Noise; δ-Doped quantum well

1. Introduction

The precise study of the material's surface magnetic structure by means of scanning Hall probe microscopy (SHPM) [1], scanning superconducting quantum interference device susceptometers (SQUID) [2] and magnetic force microscopies (MFM) [3] requires magnetic sensors of high sensitivity and signal linearity over a wide range of magnetic fields and temperatures as well as small active areas. To meet the demands of these experimental techniques, advanced III–V micro-Hall sensors with a high sensitivity, low noise, high thermal stability, and low temperature dependence are required. Modulation-doped heterostructures with high electron mobility and low electron concentration can be used to achieve very high magnetic sensitivities, but suffer from thermal drift and trapping effects which cause noise. Furthermore, the performance of these structures is very temperature dependent. In Hall devices, small enough to probe the microstructure of magnetic materials, the electric field will normally be quite large. For sensor applications with high spatial resolution, requirements include maximum signal-to-noise sensitivity (SNS), good temperature stability, and little trapping even under high electric fields.

In the last years, Hall sensors using modulation-doped AlGaAs/GaAs [4], AlAs/GaAs [5], AlGaAs/InGaAs/GaAs [6], InAlAs/InGaAs/InP [7] and Si-δ-doped AlGaAs/InGaAs/GaAs [8] or InAs/AlGaSb [9] QWs have been proposed. The high electron mobility of the 2DEG is advantageous primarily within the low-electric field region [4]. At higher electric fields ($E > 1$ kV cm^{-1}), the electron mobility in modulation-doped structures decreases significantly [5]. As a result, the supply-voltage-related sensitivity noticeably degrades. Additionally, the sheet carrier concentration in modulation-doped AlGaAs/GaAs heterostructures often increases with rising electric field, leading to a decrease in the supply-current-related sensitivity. More critical, because the mobility is

* Corresponding author. Tel.: +49-30-2093-7663; fax: +49-30-30093-7659.
E-mail address: kunets@physik.hu-berlin.de (V.P. Kunets).

0924-4247/02/$ – see front matter © 2002 Elsevier Science B.V. All rights reserved.
PII: S0924-4247(02)00197-8

highly temperature dependent in high-mobility modulation-doped structures, measurements made as a function of temperature at lower temperatures require a constant recalibration of the Hall sensor.

In this work, we describe and compare QW micro-Hall devices fabricated with uniformly Si-doped GaAs QWs in AlGaAs/GaAs heterostructures and Si-δ-doped $In_yGa_{1-y}As$:Si strained QWs in AlGaAs/GaAs/InGaAs heterostructures. We show that under larger electric fields, the signal-to-noise sensitivity is determined to a great extent by the maximum carrier velocity in the structure, and only to a lesser degree by carrier concentration and mobility. Thus, performance is optimized with materials with high electron saturation velocity, high electron concentration, and excellent materials quality leading to low 1/*f* noise. Furthermore, very good signal-to-noise performance is achievable at high electric fields due to the higher velocity at these fields. Our data further show that the 1/*f* noise also increases at higher electric fields, requiring that higher frequencies be used at higher electric fields. In our work, we achieve a maximal signal-to-noise sensitivity of 138 dB T^{-1} in a 10 μm × 10 μm device at 300 K with bandwidth of 1 Hz, corresponding to a lowest detection limit of 127 nT at a frequency of 100 kHz at an electric field of 2.4 kV cm^{-1}. We project that at higher measurement frequencies and higher fields, values of 160 dB T^{-1} $Hz^{1/2}$ and 10 nT $Hz^{1/2}$. Using the figure of merit, signal-to-noise sensitivity scaled by the width of the active region, we expect a value of 200 dB T^{-1} $Hz^{1/2}$ mm^{-1}.

2. Device fabrication

Using a Riber 32-P gas-source molecular-beam epitaxy system, $Al_{0.3}Ga_{0.7}As$/GaAs and $Al_{0.3}Ga_{0.7}As/GaAs/In_{0.3}Ga_{0.7}As$ QWs were grown on semi-insulating (0 0 1)-oriented GaAs wafers. For the group III elements Al, Ga, and In, solid sources were used; the group V element As was obtained from a AsH_3 hydride gas source, cracked at 830 °C. The surface quality was monitored by RHEED pattern both during the oxide desorption and subsequent growth. The substrate temperature was controlled using a thermocouple and an infrared pyrometer.

The epilayer sequences for the two samples primarily discussed in this paper are given in Table 1. The 1000 Å GaAs buffer layer initially grown on the substrate ensures high material and interface quality of all subsequent layers. The GaAs was grown at a growth rate of 2.0 Å s^{-1} at a growth temperature of 575 °C. The $Al_{0.3}Ga_{0.7}As$ barriers were grown at 630 °C. In structure A, a uniformly-doped GaAs:Si layer was inserted between adjacent $Al_{0.3}Ga_{0.7}$ As barriers, serving as a conductive channel for the 2DEG. The structure was capped with heavily-doped GaAs:Si, which contributes to better Ohmic contacts.

Structure B has essentially the same layer sequence as in structure A, but the addition of a 30 Å Si-δ-doped $In_yGa_{1-y}As$:Si strained QW inserted into the GaAs:Si channel layer. The δ-doping position is centered within this QW. The $In_yGa_{1-y}As$ layer was grown at a substrate temperature of 565 °C. The resulting layer thickness was kept well below the critical layer thickness (CLT) [10–15] in order to avoid misfit dislocations. Structural quality was monitored during growth using RHEED techniques.

Table 1
Structural and electronic parameters of the two samples studied

		Sample	
		A	B
GaAs:Si (cap layer)	*d* (nm)	7	7
	N_d (10^{18} cm^{-3})	2	2
$Al_{0.3}Ga_{0.7}As$ (barrier)	*d* (nm)	35	35
GaAs:Si (quantum well)	*d* (nm)	17.5	16
	N_d (10^{18} cm^{-3})	2	2
Si-δ-doped $In_{0.3}Ga_{0.7}As$ (quantum well)	*d* (nm)		3
	n_{2d} (10^{11} cm^{-2})		2.1
GaAs:Si (quantum well)	*d* (nm)	17.5	16
	N_d (10^{18} cm^{-3})	2	2
$Al_{0.3}Ga_{0.7}As$ (barrier)	*d* (nm)	35	35
GaAs:Be	*d* (nm)	10	10
	N_a (10^{18} cm^{-3})	1.5	1.5
GaAs (buffer layer)	*d* (nm)	100	100
GaAs	S.I. substrate		
Hall data (at 300 K)	n_s (10^{12} cm^{-2})	1.28	1.5
	μ_{dc} (cm^2 $V^{-1}s^{-1}$)	1651	2046

Using a standard optical photolithography, four-terminal Greek-cross micro-Hall devices with active area of 10 μm square size were fabricated. Alloying an evaporated Au:Ge:Ni metal film, Ohmic contacts were formed, with measured contact resistances of 7 and 14 Ω for Samples A and B, respectively. Chemical wet-etching was used for mesa device isolation. Varying the temperature for the thermal annealing procedure in the range of 320–450 °C, we found the optimal conditions for lowest specific resistance (20 s at 420 °C). Finally, individual chips were cut from the die, mounted and bonded on a non-magnetic chip carrier.

Both Hall mobilities and carrier concentrations in the conductive channel were also measured using the van der Pauw method in large-sized samples.

3. Magnetic sensitivity

The Hall voltage is given by

$$V_H = G\frac{IB}{en_s} \qquad (1)$$

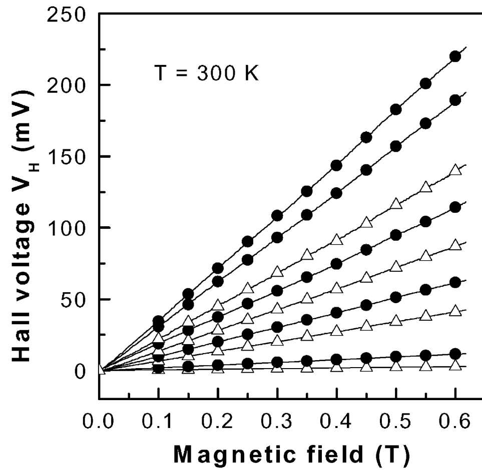

Fig. 1. Hall voltages as functions of magnetic induction in current drive mode at $T = 300$ K for different values of the bias current—(△): Sample A (10, 120, 250, and 400 μA); (●): Sample B (50, 200, 400, 800, and 1000 μA).

where I is the current, B the perpendicular magnetic field, e the electronic charge, n_s the sheet electron concentration, and G is the geometric correction factor. For our Greek-cross structures, where length of the active square is about one-third of the distance between the contacts, $G \approx 1$ [16]. Thus,

$$V_H \approx \mu EWB = vWB \quad (2)$$

where μ and v are the electron mobility and velocity, E the electric field in the active region of the Hall device, and W the width of the active (square) region. Fig. 1 shows the Hall voltage for our micro-Hall elements A and B at $T = 300$ K as function of B for various currents (and, therefore, various electric fields). Both devices exhibit an excellent linearity over an interesting range of magnetic field. The residual non-linearity of the micro-Hall device B is seen in Fig. 2 for both low and high bias currents. The estimated non-linearity does

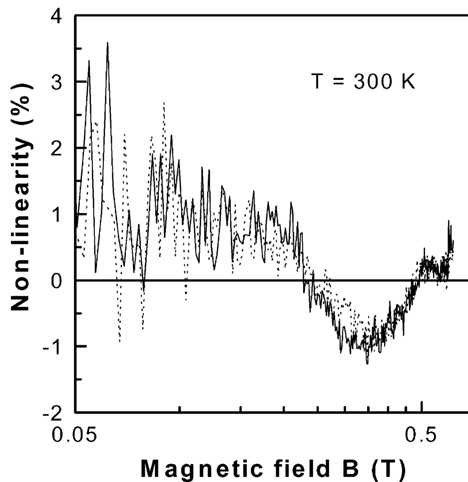

Fig. 2. Non-linearity of the Hall voltage $[(V_H(I,B) - V_{H,\,fit})/V_{H,\,fit}]$ vs. magnetic field at $T = 300$ K for Sample B: dotted line, $I = 10$ μA; full line, $I = 900$ μA.

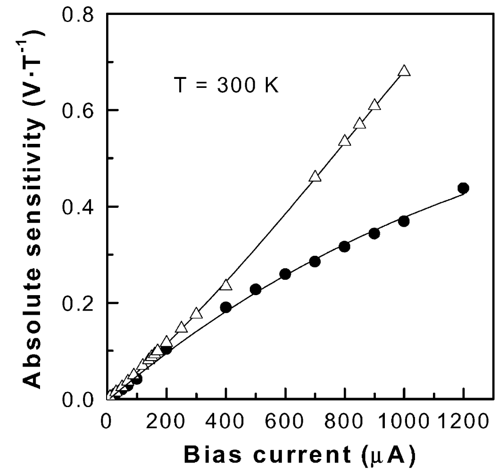

Fig. 3. Absolute sensitivity as function of bias current for Samples A and B at $T = 300$ K—(△): Sample A, (●): Sample B.

not exceed 4% and is mainly caused by measurement errors. Similar results were obtained for Sample A.

The slope of the Hall voltage plotted against B is the absolute sensitivity,

$$S_A = \frac{dV_H}{dB} \approx \mu EW = vW \quad (3)$$

Fig. 3 shows the absolute sensitivity as function of bias current for Hall devices fabricated from both structures at room temperature. For Sample A, the largest measured value of $S_A = 0.679$ V T^{-1} for a bias current of $I = 1000$ μA, corresponding to an electric field of about 5 kV cm^{-1}. For Sample B, the value of $S_A = 0.438$ V T^{-1} was measured for a current of $I = 1200$ μA corresponding to an electric field of 3.1 kV cm^{-1}.

The ratio of the absolute sensitivity to current is the current-related sensitivity,

$$S_I = \frac{1}{I}\frac{dV_H}{dB} \approx \frac{1}{n_s e} \quad (4)$$

Because of the dependence of S_I on n_s, the current-related sensitivity of Sample A is higher than that of Sample B. As will be discussed later, a low n_s has a detrimental effect on the noise. The non-constant slopes of S_A seen in Fig. 3 reflects the variations in S_I due to changes in n_s. For our micro-Hall device A, we derived best values of $S_I = 590$ V A^{-1} T^{-1} at room temperature and $S_I = 565$ V A^{-1} T^{-1} at $T = 77$ K, respectively. For Sample B, the maximum of the absolute sensitivity is found to be $S_A = 0.454$ V T^{-1} at $T = 77$ K and $S_A = 0.438$ V T^{-1} at $T = 300$ K.

Hall sensors based on modulation-doped AlGaAs/GaAs and AlAs/GaAs heterostructures can have very high values of S_I when n_s is made small; values as high as 1200 V A^{-1} T^{-1} have been reported [4,5]. Furthermore, the voltage-related sensitivity

$$S_V = \frac{1}{V}\frac{dV_H}{dB} \approx \mu \quad (5)$$

is also extremely high due the high values of the electron mobility, μ. On the other hand, DX centers are responsible for a number of disadvantages in such structures, including extremely large changes in carrier concentration at higher electric fields [5].

Structures A and B show almost no dependence of n_{2d} on temperature; the mobilities increase somewhat with increasing temperature, reflecting the positive temperature coefficient for mobility dominated by ionized impurity scattering. The 77 K mobility also increases somewhat with increasing electric field, since the electric field heats the electrons and, again, higher electron temperature leads to reduced ionized impurity scattering. The effect of the higher electric field on the carrier concentration is that it becomes somewhat smaller. This effect results in an increase in S_I. For Sample A, the low-electric field S_I is $S_I = 470\ \mathrm{V\,A^{-1}\,T^{-1}}$; this sensitivity increases between fields of 0 and $600\ \mathrm{V\,cm^{-1}}$, reaching $S_I = 590\ \mathrm{V\,A^{-1}\,T^{-1}}$ at $600\ \mathrm{V\,cm^{-1}}$ and above. At 77 K, the value of S_I varies between $S_I = 520\ \mathrm{V\,A^{-1}\,T^{-1}}$ at low fields and $S_I = 565\ \mathrm{V\,A^{-1}\,T^{-1}}$ at fields above about $1.6\ \mathrm{kV\,cm^{-1}}$. For Sample B at 300 K, the low-electric field is $S_I = 390\ \mathrm{V\,A^{-1}\,T^{-1}}$, increasing to $S_I = 520\ \mathrm{V\,A^{-1}\,T^{-1}}$ at $350\ \mathrm{V\,cm^{-1}}$, and then falling again to $S_I = 390\ \mathrm{V\,A^{-1}\,T^{-1}}$ at $1.5\ \mathrm{kV\,cm^{-1}}$. At 77 K, the value of S_I varies between $S_I = 415\ \mathrm{V\,A^{-1}\,T^{-1}}$ at low fields and $S_I = 450\ \mathrm{V\,A^{-1}\,T^{-1}}$ at fields above about $1.8\ \mathrm{kV\,cm^{-1}}$. The mechanism of free electron depletion within the QW is assumed to be a thermal or field induced trap of carriers by DX centers. The lifetime of captured carriers is normally high for these centers and depends substantially on alloy composition, electron concentration and temperature [17,18]. An estimation of this lifetime can be also derived from noise measurements as shown below.

4. Noise spectra

Measurements of voltage fluctuations across the Hall electrodes have been carried out at zero magnetic field as a function of frequency. The value of noise is expected to be the same in the low range of magnetic fields where the condition $\mu^2B^2 \ll 1$ is satisfied [7]. The measurements were made using different directions of current flow and various contacts. The typical noise spectra for our micro-Hall elements A and B at low-electric field are shown in Fig. 4.

At the lowest measured frequencies, all spectra have a tendency to show a plateau. We have measured noise spectra in a wider range of frequencies down to 0.027 Hz to confirm this tendency for our micro-Hall device B. We attribute this low-frequency noise to generation and recombination. Generation-recombination noise can be expressed as:

$$S_{V,g-r}(f) \propto \frac{1}{1 + (2\pi f\tau)^2} \tag{6}$$

where τ is the characteristic time constant. Evaluating the low-frequency data, we obtain 1.2 and 140 ms for Samples A and B, respectively. Such anomalous high magnitudes of the time constant are typical for DX centers [18].

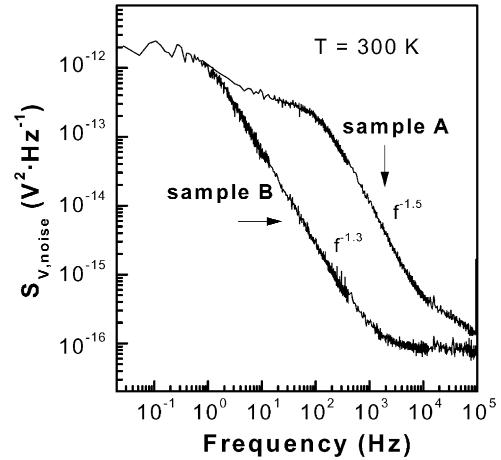

Fig. 4. Noise voltage spectra across the Hall electrodes for Samples A and B at a bias current of 10 μA at $T = 300$ K.

Between 1 Hz and about 10 kHz, the noise spectrum is dominated by flicker noise with its characteristic $1/f$ behavior. Empirically, the actual form of the noise spectral density is $1/f^n$, with $n = 1.5$ and 1.3 for Samples A and B, respectively. These curves can be fit as the sum of generation-recombination noise with its $1/f^2$ frequency dependence and flicker noise with a purely $1/f$ behavior. (Similar behavior was observed by Sugiyama et al. [5] who concluded, however, that the slope in the noise spectrum of 2DEG Hall elements was related to the processing of the Ohmic contacts.) The voltage noise spectral density for $1/f$ component of the mid-frequency noise, $S_{V,\alpha}$ across the contacts measuring the Hall voltage is given by

$$S_{V,\alpha} = \alpha E^2 (n_{2d} f)^{-1} \tag{7}$$

where α is the Hooge parameter for the material and E the applied electric field in the active area of the Hall device. Fitting the measured noise spectral density for the two devices as being the sum of generation-recombination type noise and $1/f$ noise, the Hooge parameters for the two structures were extracted. We find that for Sample A at 300 K, $\alpha = 1.5 \times 10^{-4}$ and for Sample B, also at 300 K, $\alpha = 1.1 \times 10^{-4}$. These values are typical for these materials doped as these are.

At frequencies high enough that the $1/f$ noise is small, the noise spectrum is dominated by thermal noise, which is independent of frequency. In Sample B, thermal noise dominates for frequencies above about 5 kHz; in Sample A, because of its higher $1/f$ noise, the thermal noise dominates for frequencies above about 50 kHz. The spectral noise density for thermal noise is given by

$$S_{V,\mathrm{thermal}} = 4k_{\mathrm{B}}TR \tag{8}$$

where k_{B}, T, and R are the Boltzmann constant, the absolute temperature and the resistance of the semiconductor between the two Hall voltage contacts, respectively. For

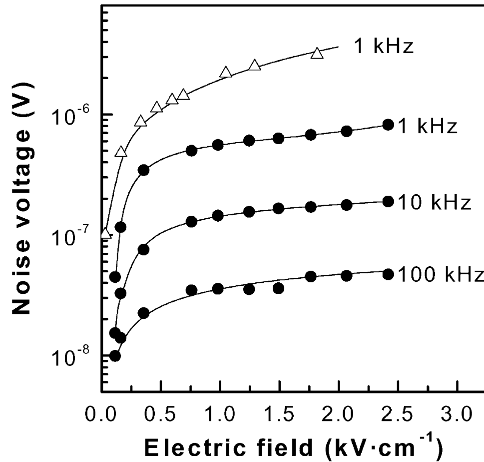

Fig. 5. Noise voltage as a function of applied electric field for micro-Hall devices A (△) and B (●), $\Delta f = 1$ Hz, $T = 300$ K.

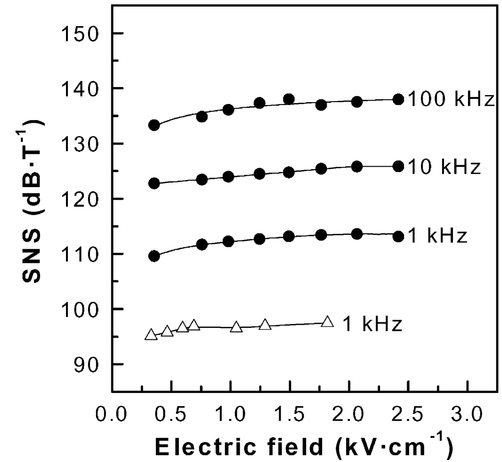

Fig. 6. Signal-to-noise sensitivity as function of applied electric field at room temperature for micro-Hall devices A (△) and B (●).

Sample B, one calculates a value of $S_{V,\mathrm{thermal}} = 8.4 \times 10^{-17}\ \mathrm{V^2\,Hz^{-1}}$, which is in excellent agreement with the measured value seen in Fig. 4. The value for Sample A is about 50% higher, but not clearly resolved still at 100 kHz.

The noise voltage in a band of frequencies, Δf, is given by

$$\bar{V}_{\mathrm{noise}} = \sqrt{S_{V,\mathrm{noise}}(f)\Delta f} \tag{9}$$

where $S_{V,\,\mathrm{noise}}$ is the voltage noise spectral density. Increasing the bias current and consequently the strength of electric field leads to an increase of noise voltage spectral density and, therefore, to the noise voltage (see Fig. 5). As long as the noise is dominated by flicker noise, the noise voltage scales approximately linearly with electric field. In fact, the noise voltage of Sample A measured at 1 kHz is proportional to E; the dependencies of Sample B are superlinear at small fields, but sub-linear at large fields. The thermal noise, on the other hand, is expected to increase only very little, due to the increase in the resistance as the velocity saturates.

The SNS sensitivity is defined as the absolute sensitivity divided by the noise voltage for a given bandwidth,

$$\mathrm{SNS} \equiv \frac{S_{\mathrm{A}}}{\bar{V}_{\mathrm{noise}}} \tag{10}$$

Its dependence on electric field is shown in Fig. 6 for several frequencies and using a measurement bandwidth of $\Delta f = 1$ Hz. Because at most electric fields, the noise is still dominated by $1/f$ noise, the SNS is approximately constant, since both S_{A} and $\bar{V}_{1/f}$ increase approximately linearly with increasing electric field.

As seen from Fig. 6, the SNS of our micro-Hall elements does not degrade even at enough high electric fields ($E > 1.5\ \mathrm{kV\,cm^{-1}}$). The maximum SNS of 80 dB $\mathrm{T^{-1}}$ at 10 Hz and 98 dB $\mathrm{T^{-1}}$ at 1 kHz for the micro-Hall device A are achieved. For the micro-Hall device B, the maximum magnitudes of SNS are 88 dB $\mathrm{T^{-1}}$ at 10 Hz, 114 dB $\mathrm{T^{-1}}$ at 1 kHz, and 138 dB $\mathrm{T^{-1}}$ at 100 kHz.

We can estimate the expected values of SNS for the two cases of $1/f$ noise and thermal noise for a cross-shaped Hall device with width W measured in the frequency band width Δf as

$$\mathrm{SNS} \approx \mu W \sqrt{\frac{f n_{\mathrm{s}}}{\alpha}} \sqrt{\frac{1}{\Delta f}} \tag{11}$$

and

$$\mathrm{SNS} \approx v W \sqrt{\frac{e n_{\mathrm{s}} \mu}{4 k_{\mathrm{B}} T}} \sqrt{\frac{1}{\Delta f}} \tag{12}$$

respectively. We see that at middle frequencies, where $1/f$ noise dominates, the SNS can be approximately constant in electric field, as long as the electron mobility remains constant. At the highest frequencies, where thermal noise dominates, the SNS can continue to increase until velocity saturation is reached. In the case of our doped structures, the electron mobility is dominated at low temperatures by ionized impurity scattering and at room temperature by both ionized impurity scattering and phonon scattering. Thus, in contrast to high-mobility structures, the mobility is relatively constant, increasing somewhat with increasing electron temperature. This effect has been seen in detailed investigations of hot electron velocity at high electric field strengths in doped quantum wells [19,20].

At the same time, the investigated structures show a decrease of the electron concentration due to trapping effect on DX centers. Consequently, the decrease of SNS is obvious (see Eqs. (11) and (12)) depending on changes of the electron concentration. Even for such an electron concentration behavior we have shown that SNS does not degrade at electric field up to 2.5 kV $\mathrm{cm^{-1}}$. Furthermore, this problem can be decided in different ways: (a) by means of using δ-doped $\mathrm{In_{0.3}Ga_{0.7}As}$ QWs spaced from the

$Al_{0.3}Ga_{0.7}As$ barrier by undoped GaAs or (b) due to the smaller Al content of δ-doped $Al_xGa_{1-x}As$/GaAs and Al_x-$Ga_{1-x}As$/GaAs/$In_yGa_{1-y}As$ heterostructures. That will be the subject of our following studies.

We estimate the detection limit at different frequencies as

$$B_{\mathrm{DL}} = \left[\frac{B_{v,\mathrm{noise}}(f)\Delta f}{S_{\mathrm{A}}^2}\right]^{1/2} = \frac{1}{\mathrm{SNS}} \tag{13}$$

The micro-Hall sensors based on $Al_xGa_{1-x}As$/GaAs heterostructures show a lowest detection limit of 103 and 14 μT at 10 and 1 kHz, respectively for a bandwidth of 1 Hz. The micro-Hall sensors with the InGaAs active channel have a lowest detection limit of 41 and 2 μT at 10 and 1 kHz, respectively.

A detailed analysis of the detection limit dependence on the applied electric field as a function of frequency is presented in Fig. 7 for our micro-Hall device B. It is clearly seen that the lowest detection limit can be achieved at higher electric fields and at higher operation frequencies. The lowest measured detection limit for a 1 Hz bandwidth is 127 nT at an operation frequency of 100 kHz and an applied electric field of 2.4 kV cm^{-1}. Since the absolute sensitivity is proportional to the electron velocity, the highest absolute sensitivity will be reached at high electric fields, when the material is in velocity saturation. For doped pseudomorphic InGaAs, this value can reach 2×10^7 cm s^{-1}, allowing an absolute sensitivity of $S_A = 2$ V T^{-1}. On the other hand, at high electric fields, the 1/*f* noise also increases, which is why the signal-to-noise sensitivity seen in Fig. 6 does not increase much with increasing electric field. The data imply, however, that at sufficiently high frequencies, also this increased 1/*f* noise falls off and only the thermal noise remains at a value of not higher than 2×10^{-8} V for a 1 Hz measurement bandwidth. Thus, for high frequencies, we anticipate a signal-to-noise sensitivity of 160 dB T^{-1} (or expressed with arbitrary bandwidth, 160 dB T^{-1} $Hz^{1/2}$) at 300 K for 10 μm × 10 μm Hall devices. For comparison purposes, a useful figure of merit is the signal-to-noise sensitivity scaled by the width of the active region. One sees from both Eqs. (11) and (12) that the SNS scales not only with $\Delta f^{-1/2}$, but also with *W*. We project that the ultimate scaled SNS for the doped-channel InGaAs is at least 200 dB T^{-1} $Hz^{1/2}$ mm^{-1}.

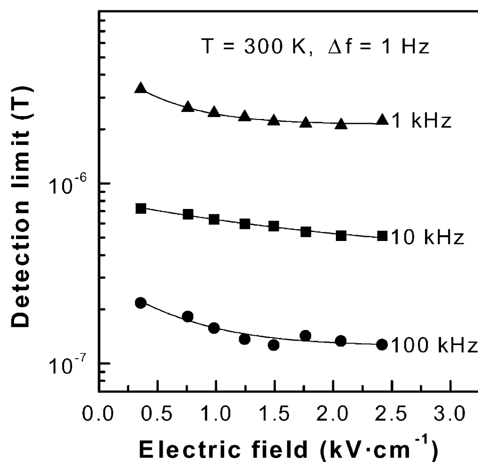

Fig. 7. Detection limit for Sample B as function of applied electric field measured at several frequencies.

5. Conclusion

Highly sensitive GaAs and InGaAs 2DEG micro-Hall devices have been fabricated from $Al_xGa_{1-x}As$/GaAs and $Al_xGa_{1-x}As$/GaAs/$In_yGa_{1-y}As$ heterostructures. These devices exhibit an excellent linearity at electric fields higher than 1.8 kV cm^{-1}. Micro-Hall elements based on Al_x-$Ga_{1-x}As$/GaAs and $Al_xGa_{1-x}As$/GaAs/$In_yGa_{1-y}As$ hetero-systems show a magnetic sensitivity of 590 and 517 V A^{-1} T^{-1} and a signal-to-noise sensitivity of 98 and 114 dB T^{-1}, respectively, not degrading even at high electric field strength. The micro-Hall devices based on Al_x-$Ga_{1-x}As$/GaAs/$In_yGa_{1-y}As$ QWs show a lower value of voltage noise spectral density in comparison with micro-Hall devices based on a $Al_xGa_{1-x}As$/GaAs heterostructure. In this case, a lowest detection limit of 127 nT at a frequency of 100 kHz and electric fields of about 2.4 kV cm^{-1} was determined, never achieved before at electric fields $E > 1.5$ kV cm^{-1}.

Acknowledgements

The authors thank B. Herrmann for Hall measurements and E. Wiebicke, A. Riedel, and E. Poblenz for technical assistance in device processing. This work was supported by the DFG Grant No. MA 1749/4-1.

References

[1] A. Oral, S.J. Bending, M. Henini, Real-time scanning Hall probe microscopy, Appl. Phys. Lett. 69 (1996) 1324–1326.

[2] C.C. Tsuei, J.R. Kirtley, C.C. Chi, L.S. Yu-Jahnes, A. Gupta, T. Shaw, J.Z. Sun, M.B. Ketchen, Pairing symmetry and flux quantization in a tricrystal superconductiong ring of $YBa_2Cu_3O_{7-\delta}$, Phys. Rev. Lett. 73 (1994) 593–596.

[3] A. Mosser, H.J. Hug, I. Parashikov, B. Stiefel, O. Fritz, H. Thomas, A. Varatoff, H.-J. Güntherodt, P. Chaudhari, Observation of single vortices condensed into a vortex-glass phase by magnetic force microscopy, Phys. Rev. Lett. 74 (1995) 1847–1850.

[4] Y. Sugiyama, T. Taguchi, M. Tacano, Highly sensitive magnetic sensor made of AlGaAs/GaAs heterojunction semiconductors, in: Proceedings of the Sixth Sensor Symposium, Japan, 1986, pp. 55–60.

[5] Y. Sugiyama, H. Soga, M. Tacano, Highly-sensitive Hall element with quantum-well superlattice structures, J. Cryst. Growth 95 (1989) 394–397.

[6] V. Mosser, S. Contreras, S. Aboulhouda, Ph. Lorenzini, F. Kobbi, J.L. Robert, K. Zekentes, High sensitivity Hall sensors with low thermal drift using AlGaAs/InGaAs/GaAs heterostructures, Sens. Actuators A 43 (1994) 135–140.

[7] S. Del Medico, T. Benyattou, G. Guillot, M. Gendry, M. Oustric, T. Venet, J. Tardy, G. Hollinger, A. Chovet, N. Mathieu, Highly sensitive $In_{0.75}Ga_{0.25}As$/AlInAs Hall sensors, Semicond. Sci. Technol. 11 (1996) 576–581.
[8] J.S. Lee, K.H. Ahn, Y.H. Jeong, D.M. Kim, Highly sensitive $Al_{0.25}Ga_{0.75}As/In_{0.25}Ga_{0.75}As$/GaAs quantum-well Hall devices with Si-δ-doped GaAs layer grown by LP-MOCVD, Sens. Actuators A 57 (1996) 183–185.
[9] M. Behet, J. Bekaert, J. De Boeck, G. Borghs, InAs/$Al_{0.2}Ga_{0.8}Sb$ quantum well Hall effect sensors, Sens. Actuators A 81 (2000) 13–17.
[10] K. Nii, R. Kuriyama, T. Hiraoka, T. Kitada, S. Shimomura, S. Hiyamizu, Larger critical thickness determined by photoluminescence measurements in pseudomorphic $In_{0.25}Ga_{0.75}As/Al_{0.32}Ga_{0.68}As$ quantum well grown on (4 1 1) GaAs substrates by molecular beam epitaxy, J. Vac. Sci. Technol. B 17 (1999) 1167–1170.
[11] W.-C. Hsu, S.-Z. Chang, W. Lin, A study of layer thickness and interface qualities of strained $In_xGa_{1-x}As$/GaAs layers, Jpn. J. Appl. Phys. 31 (1992) 26–29.
[12] M.J. Ekenstedt, S.M. Wang, T.G. Andersson, Temperature-dependent critical layer thickness for $In_{0.36}Ga_{0.64}As$/GaAs single quantum wells, Appl. Phys. Lett. 58 (1991) 854–855.
[13] T. Saeki, T. Motakawa, T. Kitada, S. Shimomura, A. Adachi, Y. Okamoto, N. Sano, S. Hiyamizu, Extremely flat interfaces in $In_xGa_{1-x}As/Al_{0.3}Ga_{0.7}As$ quantum wells grown on (411)A GaAs substrates by molecular beam epitaxy, Jpn. J. Appl. Phys. 36 (1997) 1786–1788.
[14] H. Nakao, T. Yao, Surface lattice strain relaxation at the initial stage of heteroepitaxial growth of $In_xGa_{1-x}As$ on GaAs by molecular beam epitaxy, Jpn. J. Appl. Phys. 28 (1999) L352–L355.
[15] B. Elman, E.S. Koteles, P. Melman, K. Ostreicher, C. Shung, Low substrate temperature molecular beam epitaxial growth and the critical layer thickness of InGaAs grown on GaAs, J. Appl. Phys. 70 (1991) 2634–2640.
[16] R.S. Popović, Hall Effect Devices, Adam Hilger Publishing, Bristol, 1991, pp. 165–170.
[17] A. Kastalsky, R.A. Kiehl, On the low-temperature degradation of (AlGa)As/GaAs modulation-doped field-effect transistors, IEEE Trans. Electron Devices ED-33 (1986) 414–423.
[18] P.M. Mooney, N.S. Caswell, S.L. Wright, The capture barrier of the DX center in Si-doped $Al_xGa_{1-x}As$, J. Appl. Phys. 62 (1987) 4786–4797.
[19] W.T. Masselink, T.F. Kuech, Velocity-field characteristics of electrons in doped GaAs, J. Electron. Mater. 18 (1989) 579–584.
[20] W.T. Masselink, High-differential mobility of hot electrons in δ-doped quantum wells, Appl. Phys. Lett. 59 (1991) 694–696.

Biographies

Vasyl P. Kunets was born in Kiev, Ukraine, in 1975. He received his MS degree in physics from Kiev State University in 1997. He is currently a graduate student in the Physics Department of the Humboldt University, Berlin. His research interest includes growth, electrical and optical characterization of low-dimensional system based on III–V semiconductors.

Wolfgang Hoerstel received his PhD degree in 1968 and the Dr.sc.nat. degree in 1979 both from the Humboldt University, Berlin. Since 1993, he is a scientific staff member and lecturer at the Institute of Physics in the Humboldt University, Berlin. His main interests are in electronic transport in semiconductors, especially in Te, lead salts, HgCdTe, and in the last years HgCdMnSe, and GaAs-based III–V heterostructures.

Helmar Kostial received his MS degree from the Humboldt University in Berlin, Germany in 1968 and the PhD degree from the Lomonossov State University in Moscow in 1974. Since 1992, he is a member of the scientific staff at the Paul-Drude-Institut in Berlin. During 1997 and 1998, he was a visiting guest professor at the Teikyo University in Japan. His research interests are in the physics and technology of III–V semiconductor devices, especially in the area of structuring.

Heiko Kissel received his MS degree in physics from the Humboldt University of Berlin in 1992 and is now finishing his PhD thesis on PL investigations of many-body effects in AlGaAs/InGaAs/GaAs heterostructures also at the Humboldt University. He is currently a scientific researcher in the Materials Technology Department of the Ferdinand-Braun-Institut of High-Frequency Technique. His research interests include optical properties of low-dimensional semiconductor structures, nanostructure and defect analysis as well as the development of optoelectronic devices.

Uwe Müller received his PhD degree in physics from the Humboldt University Berlin in 1990, and is working as a lecturer and scientific staff member in the Department of Physics. He has done research on SEM diagnostics and gettering in silicon MOS devices, later in FTIR-PL spectroscopy on narrow-gap semiconductors. Since 1995, his main subject is optical spectroscopy (PL, magneto-optics) on III–V heterostructures.

Georgiy G. Tarasov graduated from Kiev State University in 1967, Faculty of Radio-Physics. The PhD thesis in 1979 and the Doctor of Sciences thesis in 1989 were defended at Institute of Semiconductor Physics, National Academy of Sciences in Kiev, Ukraine. Since 1991, Dr. Tarasov is the head of Division for Laser Spectroscopy of Semiconductors and Insulating Materials at the same Institute and since 1998, he is a professor of Semiconductor and Insulator Physics. Currently, he is a visiting professor at the Humboldt University in Berlin, Germany. His main research activities are in the fields of non-linear optics, lattice dynamics of multinary compounds, superionic materials, optics of semimagnetic narrow-gap semiconductors. Recent research interests are many-body effects in quantum well heterostructures, optical and transport phenomena in low-dimensional coupled systems.

Yuriy I. Mazur received his MS degree in solid state physics from the Moscow Institute of Physics and Engineering in 1978 and the PhD degree in physics and mathematics from the Moscow Physics and Technology Institute and Institute of General Physics. Currently, he is a research assistant professor in the Department of Physics of the University of Arkansas. His research interest include optical, electrical, and magnetic properties of II–VI and III–V semiconductors and low-dimensional semiconductor structures, especially, optical and magneto-optical spectroscopy of narrow- and wide-gap semiconductors, physics of two-dimensional electron (hole) states and excitons in III–V semiconductor heterostructures and quantum dots.

Zoryana Ya. Zhuchenko graduated from Drogobych Pedagogical University in 1992, Faculty of Physics and Mathematics and received the PhD degree in 2000 for work done at the Institute of Semiconductor Physics, National Academy of Sciences, Kiev, Ukraine. She is currently a researcher at the Division for Laser Spectroscopy of Semiconductors and Insulating Materials at the same Institute. Her scientific interests include physical properties of quantum well heterostructures, III–V quantum dots and quantum wires coupled systems.

William Ted Masselink received the PhD degree in 1986 from the University of Illinois in Urbana-Champaign for work in semiconductor heterostructure physics and engineering. From 1986 to 1994, he was a research staff member at the IBM T.J. Watson Research Center in Yorktown Heights, NY. Since 1994, he is professor of physics at the Humboldt University in Berlin, Germany. He has co-authored several patent disclosures including that for the widely-used AlGaAs/InGaAs pseudomorphic field-effect transistor (pHEMT) and has authored or co-authored about 150 refereed publications.